

DISLOCATION-FREE 3D ISLANDS IN HIGHLY MISMATCHED EPITAXY: AN EQUILIBRIUM STUDY WITH ANHARMONIC INTERACTIONS

IVAN MARKOV

*Institute of Physical Chemistry, Bulgarian Academy of Sciences,
1113 Sofia, Bulgaria*

AND

JOSÉ EMILIO PRIETO

*Departamento de Física de la Materia Condensada and Instituto
Universitario de Ciencia de Materiales “Nicolás Cabrera”,
Universidad Autónoma de Madrid, 28049 Madrid, Spain*

Abstract. Accounting for the anharmonicity of the real interatomic potentials in a model in 1+1 dimensions shows that coherent 3D islands can be formed on the wetting layer in a Stranski-Krastanov growth mode predominantly in compressed overlayers. Coherent 3D islanding in expanded overlayers could be expected as an exception rather than as a rule. The thermodynamic driving force of formation of coherent 3D islands on the wetting layer of the same material is the weaker adhesion of the atoms near the islands edges. The average adhesion gets weaker with increasing island's thickness but reaches a saturation after several monolayers. A misfit greater than a critical value is a necessary condition for coherent 3D islanding. Monolayer height islands with a critical size appear as necessary precursors of the 3D islands. The 2D-3D transformation from monolayer-high islands to three-dimensional pyramids takes place through a series of stable intermediate 3D islands with discretely increasing thickness.

1. Introduction

Instabilities during growth of surfaces are of crucial importance for fabrication of devices [1]. Of particular interest in recent time is the instability of the two-dimensional (2D) layer-by-layer growth against the formation

of coherently strained (dislocation-free) three-dimensional (3D) islands of nanometer scale in highly mismatched epitaxy. The latter is known as a “coherent Stranski-Krastanov” (SK) growth [2], and is a subject of intense research owing to possible optoelectronic applications as lasers and light emitting diodes [2-4]. That is why much effort has been made in the last decade to determine the equilibrium shape of the crystallites as a function of the volume [5-8], the change of shape during growth [9], the strain distribution within the coherent islands and their energy [10-20], the kinetics of growth of arrays of quantum dots and the physical reason of the narrow size distribution [21-23], which is often experimentally observed.

The physical reason of occurrence of the Stranski-Krastanov growth mode is generally understood. Too much strain energy accumulates into the film during the initial planar growth, and the strong adhesion exerted by the substrate (which is the reason for the planar growth) disappears beyond several atomic diameters. A wetting layer (WL) composed of an integer number of equally strained monolayers is thus formed. The growth continues further by the formation of 3D crystallites, in which the additional surface energy is overcompensated by the strain relaxation. In other words, *the higher energy phase representing a homogeneously strained planar film is replaced beyond some critical thickness by a lower energy phase of (completely or partially) relaxed 3D crystallites.*

Although the essential physics seems clear, too many questions of fundamental character remain to be answered. As the atoms on top of the surface of the wetting layer do not “feel” energetically the presence of the substrate and both the wetting layer and the 3D islands consist of one and the same material, we can consider as a first approximation the formation of coherent 3D clusters in SK growth as *homoepitaxial growth* on a uniformly strained crystal surface. If so, it is not clear what is the thermodynamic driving force for 3D islanding if the islands are coherently strained to the same degree as the underlying wetting layer. This question is closely connected with the structure and energy of the boundary between the 3D islands and the wetting layer. The energy of this boundary is often taken equal to zero [13]. This means a complete wetting of the 3D islands by the substrate (the WL) which rules out the 3D islanding from a thermodynamic point of view. It is also not clear why coherent 3D islands are observed in compressed rather than in expanded overlayers, and at values of the misfit $\varepsilon_0 = \Delta a/a$ that are huge for materials with directional and brittle covalent bonds (InAs/InP (3.2%) [24], Ge/Si (4.2%) [2, 25], InAs/GaAs (7.2%) [26], CdSe/ZnSe (7.6%) [27]). The only exception, to the authors’ knowledge, of expanded overlayer, is the system PbSe/PbTe (-5.5%) [28]. Other question is whether the misfit should be greater than some critical value in order for the coherent 3D islanding to take place. Are two-dimensional monolayer

height islands necessary precursors for the formation of 3D islands as suggested by some authors [14, 17, 29, 30]? If yes, is there a critical volume size (or a size of the 2D island) for the 2D-3D transformation to occur? What is the pathway of the latter, does it pass through a series of intermediate states with increasing thickness, and are these states stable or metastable? In this paper we make an attempt to answer at least qualitatively some of the questions posed above.

The thermodynamic driving force for occurrence of one or another mode of growth should be given by the difference $\Delta\mu = \mu(n) - \mu_{3D}^0$ of the chemical potentials $\mu(n)$ of the film, and μ_{3D}^0 of the bulk crystal of the same material. The film chemical potential depends on the thickness measured in number n of monolayers owing to the thickness distribution of the misfit strain and the attenuation of the energetic influence of the substrate [31-33]. If we deposit a crystal A on the surface of a crystal B the thermodynamic driving force can be written in terms of interatomic energies $\Delta\mu = E_{AA}\Phi$ where $\Phi = 1 - E_{AB}/E_{AA}$ is the so-called adhesion parameter which accounts for the wetting of the substrate by the overgrowth [34]. E_{AA} and E_{AB} are the energies per atom to disjoin a half-crystal A from a like half-crystal A and from an unlike half-crystal B , respectively. E_{AB} is in fact the adhesion energy which includes in itself the thickness distribution of the strain energy due to the lattice misfit, and the attenuation of the bonding with the substrate [31, 35]. The adhesion parameter Φ is the same which accounts for the influence of the substrate on the work of formation of 3D nuclei of different material on top of it in the classical nucleation theory [35]. Replacing the bonding energies E_{AA} and E_{AB} by the corresponding surface energies gives the famous 3- σ criterion of Bauer for the mode of growth $\Delta\mu = a^2[\sigma_A + \sigma_{AB}(n) - \sigma_B]$ [36], where a^2 is the area occupied by an atom at the interface.

The thickness dependence of the film chemical potential is schematically illustrated in Fig. 1. In the two limiting cases of Volmer-Weber (VW) (incomplete wetting, $0 < \Phi < 1$) and Frank-van der Merwe (FM) growth (complete wetting, $\Phi \leq 0, \varepsilon_0 \cong 0$) $\mu(n) - \mu_{3D}^0$ goes asymptotically to zero from above and from below, respectively, but changes sign in the case of SK growth ($\Phi \leq 0, \varepsilon_0 \neq 0$) [31, 32, 35, 37]. In the latter case, beyond the maximum, we consider the 3D islands as the overlayer material A , and the wetting layer as the substrate crystal B . Thus the strained wetting layer and the relaxed 3D islands represent necessarily different phases in the sense of Gibbs. The wetting layer can be in equilibrium only with an *undersaturated vapor phase*, whereas the 3D islands are in equilibrium with a *supersaturated vapor*. The dividing line is $\Delta\mu = 0$ at which the wetting layer cannot grow thicker and the 3D islands cannot nucleate and grow. Thus the adhesion parameter $\Phi = \Delta\mu/E_{AA}$ relative to the cohesion energy

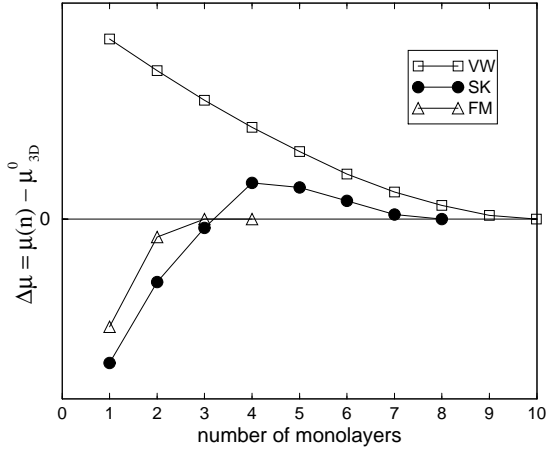


Figure 1. Schematic dependence of the thermodynamic driving force $\Delta\mu = \mu(n) - \mu_{3D}^0$ which determines the occurrence of a given mode of growth on the film thickness in number of monolayers: VW - Volmer-Weber, SK - Stranski-Krastanov, and FM - Frank-van der Merwe. Note that in the case of FM growth the points denote the chemical potentials of the separate monolayers as only the uppermost incomplete monolayer determines the equilibrium vapor pressure. In the other extreme of VW growth, all monolayers are incomplete and the chemical potential will be given by the mean value of the chemical potentials of all constituent monolayers. This fact was realized by Stranski and Krastanov themselves in their seminal paper (Sitzungsber. Akad. Wissenschaft Wien **146**, 797 (1938), see for review Refs. [33,35]).

E_{AA} is in fact equal to the thermodynamic driving force for the occurrence of one or another mode of growth. In other words, we can treat the SK mode as a FM mode driven by complete wetting ($\Delta\mu < 0$), followed by VW mode driven by incomplete wetting ($\Delta\mu > 0$). (The more rigorous definition is $d\mu/dn < 0$ or $d\mu/dn > 0$ [32]). The question is how the lattice misfit can lead to incomplete wetting ($\Phi > 0$) on the surface of the wetting layer if the energetic influence exerted by the substrate is already lost, i.e. $E_{AB} \rightarrow E_{AA}$. In the classical SK mode the incomplete wetting is due to the introduction of misfit dislocations (MDs) [38]. Once we know the answer of this question in the case of a coherent SK growth we could easily find the answers of the others.

2. Model

We consider an atomistic model in 1 + 1 dimensions (substrate + height) which we treat as a cross section of the real 2 + 1 case. An implicit assumption is that in the real 2 + 1 model the monolayer islands have a compact rather than a fractal shape and the lattice misfit is one and the same in both orthogonal directions. Furthermore, we exclude from our considera-

tions the possible interdiffusion and the subsequent gradient of strain as found recently by Kegel *et al* [39] in the case of InAs/GaAs quantum dots. The 3D islands are represented by linear chains of atoms stacked one upon the other as in the model proposed by Stoop and van der Merwe [40] and later by Ratsch and Zangwill [12], each upper chain being shorter than the lower one by one atom. In this sense the lateral size, and particularly the height of the islands are *discrete* parameters, whereas in most of the theoretical considerations they are taken as continuous variables [1, 5, 13].

In a previous paper [30], we used the method of computation proposed by Ratsch and Zangwill [12], which is based on the well-known model of Frenkel and Kontorova [41]. The latter treats the overlayer as a linear chain of atoms subject to an external periodic potential exerted by a rigid substrate [41, 42]. Ratsch and Zangwill accepted that each layer (chain) presents a rigid sinusoidal potential to the chain of atoms on top of it. The potential trough separation of the lower chain is taken constant and equal to the average of all trough separations. As the strains of the bonds that are closer to the free ends are smaller, the average bond strain of each upper chain is closer to zero. In other words, the lattice misfit decreases from ε_0 at the island's base to zero at the apex. This method is, however, inadequate to describe properly a thickening overlayer because of one basic assumption, namely, the rigidity of each monolayer upon formation of the next one on top of it. This assumption rules out the relaxation and redistribution of the strains in the lower layers when upper layers are added. In particular, this method does not allow to compute the structure and energy of the interfacial boundary between the wetting layer and the 3D islands upon thickening of the latter.

For the above-mentioned reasons, in the present work we make use of a simple minimization procedure. The atoms interact through a Morse potential that can be easily generalized to vary its anharmonicity by adjusting two constants μ and ν ($\mu > \nu$) that govern separately the repulsive and the attractive branches, respectively [44-46],

$$V(x) = V_o \left[\frac{\nu}{\mu - \nu} e^{-\mu(x-b)} - \frac{\mu}{\mu - \nu} e^{-\nu(x-b)} \right], \quad (1)$$

where b is the equilibrium atom separation. For $\mu = 2\nu$ the potential (1) turns into the familiar Morse potential, which has been used in the present work for the case $\nu = 6$.

The pair potential designed by Tersoff for description of the properties of materials with directional covalent bonds like Si contains an additional parameter which accounts for the local atomic environments around the neighboring atoms [44]. He showed that most of the properties of Si could be computed with an error smaller than 1%, compared with experimental

data and *ab initio* calculations, by accounting only for the first neighbor interactions. For this reason, we occasionally consider only interactions in the first coordination sphere in order to mimic the directional bonds that are characteristic for the most semiconductor materials.

Our programs calculate the interaction energy of all the atoms as well as its gradient with respect to the atomic coordinates, i.e. the forces. Relaxation of the system is performed by allowing the atoms to displace in the direction of the gradient in an iterative procedure until the forces fall below some negligible cutoff value. The calculations were performed under the assumption that the substrate (the wetting layer) is rigid. This assumption is strictly valid in the beginning of the 2D-3D transformation when the 3D islands are still very thin [43].

Yu and Madhukar computed recently, by making use of the Stillinger-Weber interatomic potential [47] in a molecular dynamics study, the distribution of the strains and stresses in and around a 3D Ge island having a shape of a full pyramid with a length of the base edge 326 Å and a height of 23 monolayers [19]. They found that the atoms in the middle of the first atomic plane of a coherent 3D Ge island are displaced upwards by 0.6 Å that is approximately half of the interplanar spacing of Ge(001) (1.4 Å), whereas the atoms at the island's edges are displaced slightly downwards. The same holds for the vertical displacements of the atoms belonging to the uppermost Si plane. As the vertical displacements strongly influence the adhesion of the islands to the wetting layer we also performed preliminary calculations in which the uppermost three monolayers were allowed to relax. The results of these calculations demonstrated qualitatively the same behavior as in the case of a rigid substrate. For this reason, we present here only the results obtained under the assumption of the rigid substrate. Detailed systematic studies of the effect of the substrate relaxation will be published elsewhere.

3. Results

Fig. 2(a) shows the horizontal displacements of the atoms of the base chain of a coherently strained island, for a value of the misfit of 7%. The displacements are referenced to the sites the atoms would occupy if they belonged to the next complete monolayer, which would then be a part of the wetting layer. It can be seen that the end atoms are strongly displaced as in the model of Frenkel and Kontorova [41] and of Frank and van der Merwe [42]. Increasing the island height leads to greater displacements of the end atoms. The reason is the effective increase of the strength of the lateral interatomic bonding in the overlayer with greater thickness as predicted by van der Merwe *et al.* [43]. According to these authors an island

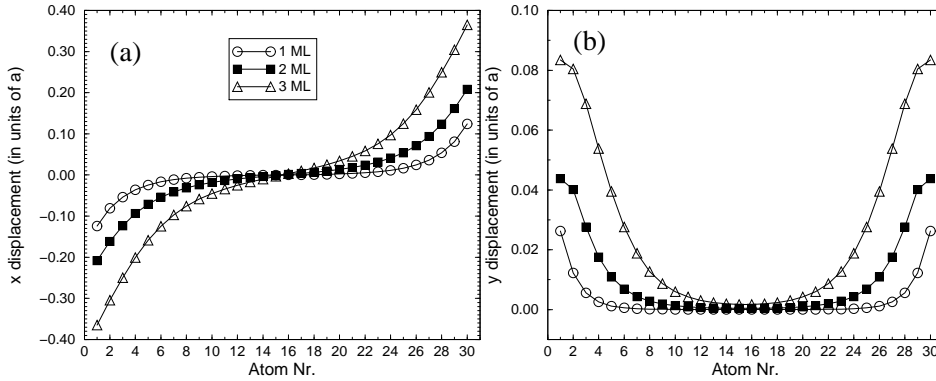


Figure 2. Horizontal (a) and vertical (b) displacements of the atoms of the base chain from the bottoms of the potential troughs provided by the homogeneously strained wetting layer for a misfit of 7%. The displacements are given in units of a , the lattice parameter of the substrate and wetting layer. They increase with increasing island's thickness taken in number of monolayers. Islands of 30 atoms in the base chain were considered.

with a bilayer height could be approximately simulated by a monolayer height island but with twice stronger lateral bonds. Fig. 2(b) shows the vertical displacements of the base atoms relative to the interplanar spacing between the monolayers belonging to the wetting layer. It is obvious that the vertical displacements are due to the climbing of the atoms on top of underlying atoms as a result of the horizontal displacements. The thicker the islands the greater are the horizontal displacements (for reasons discussed above) and in turn the vertical displacements. The results shown in Fig. 2 clearly demonstrate that the bonds that are close to the island's edges are much less strained compared with these in the middle, in agreement with the results obtained by Ashu and Matthai [10] and Orr *et al.* [11] but contrary to the finding of Yu and Madhukar [19].

The interconnection between the vertical and the horizontal displacements is beautifully demonstrated in Fig. 3 where they are shown in an island containing two MDs. The horizontal displacements in this case are greatest in the cores of the MDs and so are the vertical displacements. This figure shows in fact the physical reason for the incomplete wetting in the classical SK mode. The adhesion is weaker owing to the introduction of MDs.

In order to illustrate the effect of the atom displacements on the adhesion of the separate atoms belonging to the island's base chain, we plot their energy of interaction with the underlying wetting layer (Fig. 4) for coherently strained islands. As seen the atoms that are near to the chain ends (island's edges) adhere much more weakly with the substrate. The influence of the potential anharmonicity is clearly demonstrated. Only one

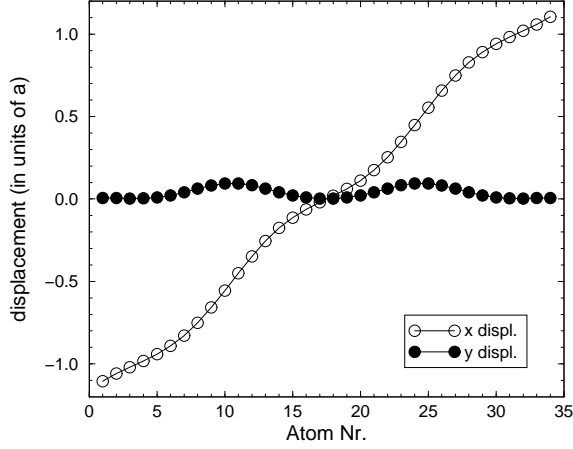


Figure 3. Horizontal (x) and vertical (y) displacements of the atoms of the base chain of an island three monolayers thick and containing two MDs. The island contains a total amount of 99 atoms (34 in the base chain) and the lattice misfit is 7%.

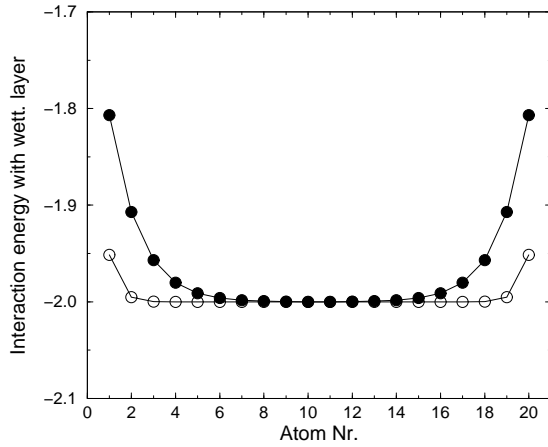


Figure 4. Distribution of the energy (in units of V_o) of first-neighbors interaction, $E_{AB}(n)$, between the atoms of the base chain (A) of a monolayer-high, coherent island consisting of 20 atoms, and the underlying wetting layer, B , for positive (\bullet) and negative (\circ) misfits of absolute value 7%.

or two end atoms in the expanded chain adhere more weakly to the substrate whereas more than half of the atoms at both ends in the compressed chain are weakly bound. The figure demonstrates in fact the physical reason for the coherent SK mode which is often overlooked in theoretical models. Moreover, it is a clear evidence of why compressed rather than expanded overlayers exhibit greater tendency to coherent SK growth.

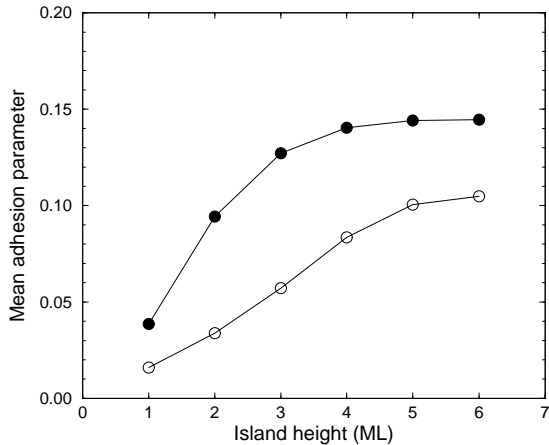


Figure 5. Mean adhesion parameter Φ as a function of the islands' height in number of monolayers for positive (●) and negative (○) values of the misfit of absolute value of 7%. Coherent islands of 14 atoms in the base chain were considered in the calculations.

It follows from Fig. 2 that increasing the island thickness leads to weaker adhesion of the 3D islands to the wetting layer and, in turn, to the stabilization of the coherent 3D islands. This is clearly demonstrated in Fig. 5 which shows the dependence of the mean adhesion parameter Φ on the islands' height for positive and negative values of the misfit. It is calculated as the average of the interaction energy between the base chain atoms and those of the wetting layer and is referenced to the corresponding value for a non-misfitting monolayer of the same size. It can be seen that Φ saturates beyond a thickness of about 5 monolayers as expected. Note that in this case the incomplete wetting ($\Phi > 0$) is due solely to the misfit, the bonding in both phases *A* (the wetting layer) and *B* (the 3D islands) being nearly one and the same. What is more important is that the adhesion parameter in compressed islands is visibly larger than that in expanded islands which is due to the anharmonicity of the interatomic potential. This behavior clearly shows the greater tendency of the compressed overlayers to form coherent 3D islands. Another important feature that characterizes the mean adhesion parameter is its large absolute value. It is comparable with the values that lead to 3D islanding in VW mode of growth on chemically unlike surfaces [35].

Fig. 6 shows the mean adhesion parameter Φ as a function of the misfit both negative and positive for coherent islands as well as for islands containing one and two MDs. As discussed in the Introduction this is in fact the thermodynamic driving force for 3D islanding. Several interesting properties are observed. First, the mean adhesion parameter of compressed

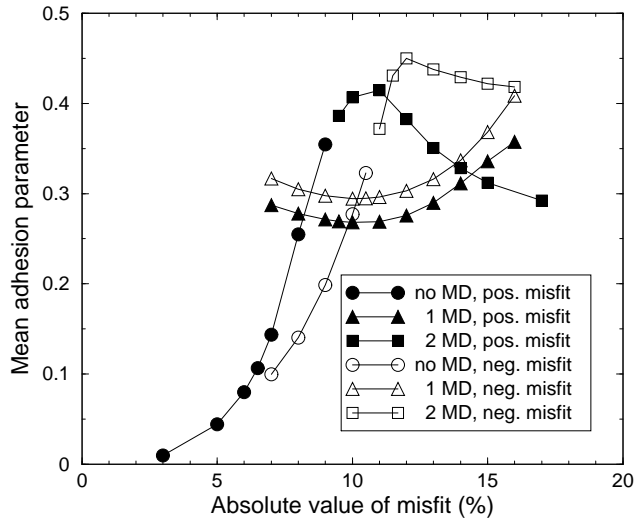


Figure 6. Mean adhesion parameter as a function of the lattice misfit. The points correspond to the saturated values from curves as those shown in Fig. 5 for coherent islands and, in addition, for islands containing one and two MDs. The islands contain 14 atoms in the base chain and have a height of 5 ML. Data for both positive and negative misfits are shown in one quadrant for easier comparison.

coherent islands is greater than that of expanded islands. This means that the thermodynamic driving force for coherent 3D islanding is greater in compressed rather than in expanded overlayers. In the absence of MDs the incomplete wetting is due to the displacements of the end atoms (see Fig. 2). In expanded overlayers the end atoms interact with their neighbors by the weaker attractive branches and *vice versa*. As a result $\Phi_0^+ > \Phi_0^-$.

On the other hand, the opposite is observed for dislocated islands. This is very easy to understand bearing in mind that in the classical (dislocated) SK mode $E_{AB} \approx E_{AA} - E_{MD}$, and $\Phi \approx E_{MD}/E_{AA}$ [35], E_{MD} being the energy per atom of the MDs. MDs have higher energy in expanded overlayers as they represent regions with higher density of atoms which repulse each other with the stronger repulsive branches of the potential. It is exactly the opposite in compressed overlayers, so that $E_{MD}^+ < E_{MD}^-$ and $\Phi_{MD}^+ < \Phi_{MD}^-$. This means that in the classical SK growth the thermodynamic driving force of formation of dislocated 3D islands is greater in expanded rather than in compressed overlayers.

Another property is that the adhesion parameter of islands containing two MDs appears as a continuation of that of the dislocation-free islands. This is also easily understandable having in mind the similarity of the model with that of Frank and van der Merwe [42]. Dislocation-free solutions

exist until the misfit reaches the so-called *metastability limit* at which the end atoms reach the crests between the next potential troughs and two dislocations (because of the symmetry of the model) are simultaneously introduced at both free ends. The energetic barrier for this process is equal to zero (for a review see Ref. ([35]).

In order to answer the questions posed in the Introduction we compare the energies per atom of mono- and multilayer islands (frustums of pyramids) with different thickness varied by one monolayer. The pyramids are bounded with the steepest (60°) sidewalls as they have the lowest energy in models in $1 + 1$ dimensions [12, 30]. As calculated, the energy represents a sum of the strain energy and the energy of the surfaces relative to the energy of the same number of atoms in the bulk crystal [29, 30]. Fig. 7(a) demonstrates the energies per atom vs the total number of atoms of monolayer and bilayer height islands at $\varepsilon_0 = 0.03$. As seen the monolayer height islands are always stable against the bilayer islands. The latter means that the thermodynamics do not favor coherent 3D islanding. Monolayer height islands will grow and coalesce until they cover the whole surface. MDs will be then introduced to relieve the strain. Fig. 7(b) demonstrates the same dependence (including also thicker islands) but at larger value of the misfit $\varepsilon_0 = 0.07$. This time the behavior is completely different. The monolayer islands are stable against the bilayer islands only upto a critical volume N_{12} , the bilayer islands are stable in turn against the trilayer islands upto a second critical volume N_{23} , etc. This behavior is precisely the same as in the case of VW growth where the interatomic forces (the wetting) predominate and the lattice misfit plays an additional role [29]. The same result (not shown) has been obtained in the case of expanded overlayers ($\varepsilon_0 < 0$) with the only exception that monolayer height islands are stable against multilayer islands upto much larger absolute values of the misfit.

The mono-bilayer transformation is the first step of the complete 2D-3D transformation. Studying the critical size N_{12} as a function of the misfit (see Fig. 8) shows the existence of critical misfits beyond which the formation of multilayer islands can only take place. Below the critical misfit the monolayer height islands are stable irrespective of their size and the growth will continue in a layer-by-layer mode until MDs are introduced to relax the strain. The nearly twice larger absolute value of the negative critical misfit is obviously due to the anharmonicity of the atomic interactions. The weaker attractive interatomic forces lead to smaller displacements both lateral and vertical of the end atoms and in turn to stronger adhesion. The latter requires larger misfit in order for the 3D islanding to take place.

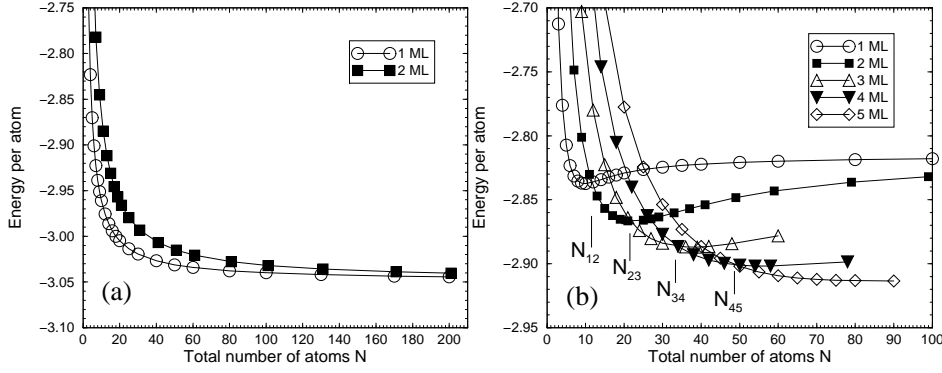


Figure 7. Dependence of the total energy per atom, in units of V_o , on the total number of atoms in compressed, coherently strained islands of different thicknesses, for two different values of the misfit: (a) $\varepsilon_0 = 0.03$, (b) $\varepsilon_0 = 0.07$. The numbers N_{12} , N_{23} , etc. give the limits of stability of monolayer, bilayer, ... islands, respectively.

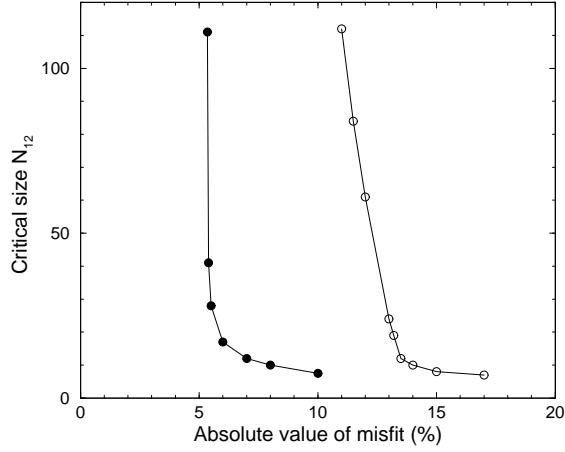


Figure 8. Misfit dependence of the critical size N_{12} (in number of atoms) for positive (●) and negative (○) values of the lattice misfit. The curves are shown in one quadrant for easier comparison.

4. Discussion

The existence of critical misfit clearly shows that the origin of the 3D islanding in the coherent SK growth is the incomplete wetting which is due to the atomic displacements near the islands edges. As seen in Fig. 6 the mean adhesion parameter Φ , or which is the same, the thermodynamic driving force $\Delta\mu$ for coherent 3D islanding has practically the same values as that in the case of the classical (dislocated) SK mode at sufficiently large values of the misfit. Moreover, the comparison of Fig. 2 and Fig. 3 shows

that at a given misfit and a given thickness, there is a critical lateral size (or a critical volume) beyond which MDs are spontaneously introduced to relieve the strain. It in fact determines the transition from the coherent to the classical (dislocated) SK growth which in the real case should be accompanied with the change of the shape. All the above leads to the conclusion that the physical reason for both the classical and coherent SK mode is one and the same.

The average adhesion depends strongly on the anharmonicity of the interatomic forces. Expanded islands adhere more strongly to the wetting layer and the critical misfit beyond which coherent 3D islanding is possible is much greater in absolute value compared with that in compressed overlayers. As a result coherent SK growth in expanded films could be expected at very (unrealistically) large absolute values of the negative misfit. The latter, however, depends on the materials parameters (degree of anharmonicity, strength of the chemical bonds, etc.) of the particular system and cannot be completely ruled out. Xie *et al* [48] studied the deposition of $\text{Si}_{0.5}\text{Ge}_{0.5}$ films in the whole range of 2% tensile to 2% compressive misfit on relaxed buffer layers of $\text{Si}_x\text{Ge}_{1-x}$ starting from $x = 0$ (pure Ge) to $x = 1$ (pure Si). They found that 3D islands are formed only under compressive misfit larger than 1.4%. Films under tensile misfit were thus stable against 3D islanding in excellent agreement with the predictions of our model.

The existence of a critical misfit for 2D-3D transformation to occur both in compressed and expanded overlayers has been noticed in practically all systems studied so far. Pinczolis *et al.* [28] have found that deposition of $\text{PbSe}_{1-x}\text{Te}_x$ on $\text{PbTe}(111)$ remains purely two dimensional when the misfit is less than 1.6% in absolute value (Se content < 30%). Leonard *et al.*[3] have successfully grown quantum dots of $\text{In}_x\text{Ga}_{1-x}\text{As}$ on $\text{GaAs}(001)$ with $x = 0.5$ ($\varepsilon_0 \approx 3.6\%$) but 60Å thick 2D quantum wells at $x = 0.17$ ($\varepsilon_0 \approx 1.2\%$). Walther *et al.* [49] found that the critical In content is approximately $x = 0.25$, or $\varepsilon_0 \approx 1.8\%$. As commented before, a critical misfit of 1.4% has been found by Xie *et al* upon deposition of $\text{Si}_{0.5}\text{Ge}_{0.5}$ films on relaxed buffer layers of $\text{Si}_x\text{Ge}_{1-x}$ with varying composition [48].

A rearrangement of monolayer height (2D) islands into multilayer (3D) islands has been reported by Moison *et al.* [26] who established that the 3D islands of InAs begin to form on GaAs at a coverage of about 1.75 ML but then the latter suddenly decreases to 1.2 ML. This decrease of the coverage in the second monolayer could be interpreted as a rearrangement of an amount of nearly half a monolayer into 3D islands. The same phenomenon has been noticed by Shklyae, Shibata and Ichikawa in the case of $\text{Ge/Si}(111)$ [50]. Voigtländer and Zinner noted that Ge 3D islands in $\text{Ge/Si}(111)$ epitaxy have been observed at the same locations where 2D islands locally exceeded the critical wetting layer thickness of 2 bilayers [51].

Bhatti *et al.* [52] and Polimeni *et al.* [53] also reported the coexistence of large pyramids and small flat islands. These observations show that the 2D islands really appear as precursors for the 3D islands.

The question of the existence and particularly the stability of the intermediate states is more difficult to answer. Rudra *et al.* measured photoluminescence (PL) spectra of InAs layers deposited on InP(001) at two different temperatures (490 and 525°C) and buried in the same material [24]. When the layers were grown at 490°C and the capping layer was deposited immediately after the deposition of the InAs the spectrum consisted of a single line. If the InAs layer was annealed for 10 s before capping with InP the spectrum consisted of 8 lines. At 525°C 3 lines were observed already in absence of annealing. The above observations could be explained by formation and coexistence of islands with different thickness varying by one monolayer. Colocci *et al.* [54] performed PL studies of InAs deposits on GaAs(001) with thickness slightly varying around the critical thickness of 1.6 monolayers for the onset of the 3D islanding. They observed an increasing number of luminescence lines with increasing film thickness. These lines were attributed to families of 3D islands with similar shape but with heights differing by one monolayer. Flat platelets, 2 - 6 monolayers high, have been observed during the growth of GaN/AlN heterostructures [55].

Although the above results seem to be in an excellent qualitative agreement with the theoretical predictions of the model, the thermodynamic stability of islands with quantized height of one monolayer, and the existence of a critical misfit is still debated [1, 5]. The reason of the discrepancy of our results with those of Duport *et al.* [5] most probably stems from the implicit assumption, made by the above authors, that the widths of the lower, R , and the upper, R' , bases, and particularly the height h , of the crystal having a shape of a frustum of a pyramid, they consider, are continuous variables. This is correct if the crystals are sufficiently large. However, the continuum approximation is not acceptable in the beginning of the 2D-3D transformation when the islands are still very small (and thin). It is also not applicable in the limit $h \ll R$ for the same reasons. The question of existence of a critical misfit follows logically if we accept that the intermediate states with heights differing by one monolayers exist and are thermodynamically stable in consecutive intervals of the volume.

In conclusion, accounting for the anharmonicity of the real interatomic potentials in a model in $1 + 1$ dimensions, we have shown that coherent 3D islands can be formed on the wetting layer in the SK mode predominantly in compressed overlayers. Coherent 3D islanding in expanded overlayers could be expected as an exception rather than as a rule. The thermodynamic driving force for 3D islanding on the wetting layer of the same material is identified as the weaker adhesion of the atoms near the islands edges. This

should also facilitate the 2D-3D transformation. Overcoming a critical lattice misfit appears as a necessary condition for the formation of coherent 3D islands. Monolayer height islands of a critical size appear as necessary precursors of the 3D islands. The 2D-3D transformation from monolayer islands to 3D pyramids takes place through a series of intermediate states with heights increasing by one monolayer. The intermediate states are thermodynamically stable in consecutive intervals of the volume.

Acknowledgements

The authors are indebted to the Instituto Universitario de Ciencia de Materiales “Nicolás Cabrera” for granting research visits which enabled scientific collaboration. This work was supported by the Spanish CICYT through project Nr. MAT98-0965-C04-02.

References

1. P. Politi, G. Grenet, A. Marty, A. Ponchet, and J. Villain, *Phys. Rep.* **324**, 271 (2000).
2. D. J. Eaglesham and M. Cerullo, *Phys. Rev. Lett.* **64**, 1943 (1990).
3. D. Leonard, M. Krishnamurthy, C. M. Reaves, S. P. Denbaars, and P. M. Petroff, *Appl. Phys. Lett.* **63**, 3203 (1993).
4. Vinh Le Thanh, P. Boucaud, D. Débarre, Y. Zheng, D. Bouchier, and J.-M. Lourtioz, *Phys. Rev B* **58**, 13 115 (1998).
5. C. Dupont, C. Priester, and J. Villain, in *Morphological Organization in Epitaxial Growth and Removal*, Vol. 14 of *Directions in Condensed Matter Physics*, edited by Z. Zhang and M. Lagally (World Scientific, Singapore, 1998).
6. B. J. Spencer and J. Tersoff, *Phys. Rev. Lett.* **79**, 4858 (1997); B. J. Spencer, *Phys. Rev. B* **59**, 2011 (1999).
7. Q. K. K. Liu, N. Moll, M. Scheffler, and E. Pehlke, *Phys. Rev. B* **60**, 17 008 (1999).
8. P. Müller and R. Kern, *Surf. Sci.* **457**, 229 (2000).
9. I. Daruka, J. Tersoff and A.-L. Barabási, *Phys. Rev. Lett.* **82**, 2753 (1999).
10. P. Ashu and C. C. Matthai, *Appl. Surf. Sci.* **48/49**, 39 (1991).
11. B. G. Orr, D. Kessler, C. W. Snyder, and L. Sander, *Europhys. Lett.* **19**, 33 (1992).
12. C. Ratsch and A. Zangwill, *Surf. Sci.* **293**, 123 (1993).
13. J. Tersoff and R. M. Tromp, *Phys. Rev. Lett.* **70**, 2782 (1993).
14. C. Priester and M. Lannoo, *Phys. Rev. Lett.* **75**, 93 (1995).
15. I. Daruka and A.-L. Barabási, *Phys. Rev. Lett.* **79**, 3708 (1997).
16. V. A. Shchukin, N. N. Ledentsov, P. S. Kop'ev, and D. Bimberg, *Phys. Rev. Lett.* **75**, 2968 (1995).
17. Y. Chen and J. Washburn, *Phys. Rev. Lett.* **77**, 4046 (1996).
18. L. B. Freund, H. T. Johnson, and R. V. Kukta, *Mat. Res. Soc. Symp. Proc.*, vol. 399, edited by A. Zangwill, D. Jesson, D. Chambliss, and R. Clarke, 1996, p. 359.
19. W. Yu and A. Madhukar, *Phys. Rev. Lett.* **79**, 905 (1997).
20. L. G. Wang, P. Kratzer, M. Scheffler, and N. Moll, *Phys. Rev. Lett.* **82**, 4042 (1999).
21. B. A. Joyce, J. L. Sudijono, J. G. Belk, H. Yamaguchi, X. M. Zhang, H. T. Dobbs, A. Zangwill, D. D. Vvedensky, and T. S. Jones, *Jpn. J. Appl. Phys.* **36**, 4111 (1997).
22. H. T. Dobbs, D. Vvedensky, A. Zangwill, J. Johansson, N. Carlsson, and W. Seifert, *Phys. Rev. Lett.* **79**, 897 (1997).
23. H. M. Koduvally and A. Zangwill, *Phys. Rev. B* **60**, R2204 (1999).

24. A. Rudra, R. Houdré, J. F. Carlin, and M. Ilegems, *J. Cryst. Growth* **136**, 278 (1994); R. Houdré, J. F. Carlin, A. Rudra, J. Ling, and M. Ilegems, *Superlattices and Microstructures* **13**, 67 (1993).
25. Y.-W. Mo, D. E. Savage, B. S. Swartzentruber, and M. Lagally, *Phys. Rev. Lett.* **65**, 1020 (1990).
26. J. M. Moison, F. Houzay, F. Barthe, L. Leprince, E. André, and O. Vatel, *Appl. Phys. Lett.* **64**, 196 (1994).
27. D. Schikora *et al.*, *Appl. Phys. Lett.* **76**, 418 (2000); M. Strassburg *et al.*, *Appl. Phys. Lett.* **76**, 685 (2000).
28. M. Pinzolit, G. Springholz, and G. Bauer, *Appl. Phys. Lett.* **73**, 250 (1998).
29. S. Stoyanov and I. Markov, *Surf. Sci.* **116**, 313 (1982).
30. E. Korutcheva, A. M. Turiel, and I. Markov, *Phys. Rev. B* **61**, 16 890 (2000).
31. R. Kern, G. LeLay, and J. J. Metois, in *Current Topics in Materials Science*, vol. 3, ed. by E. Kaldis, (North-Holland, 1979).
32. S. Stoyanov, *Surf. Sci.* **172**, 198 (1986).
33. I. Markov and S. Stoyanov, *Contemp. Phys.* **28**, 267 (1987).
34. R. Kaischew, *Commun. Bulg. Acad. Sci. (Ser. Phys.)* **1**, 100 (1950); *Fortschr. Miner.* **38**, 7 (1960).
35. I. Markov, *Crystal Growth for Beginners, Fundamentals of Nucleation, Crystal Growth and Epitaxy*, (World Scientific, Singapore, 1995).
36. E. Bauer, *Z. Kristallogr.* **110**, 372 (1958).
37. M. H. Grabow and G. H. Gilmer, *Surf. Sci.* **194**, 333 (1988).
38. J. W. Matthews, D. C. Jackson, and A. Chambers, *Thin Solid Films* **29**, 129 (1975).
39. I. Kegel, T. H. Metzger, A. Lorke, J. Peisl, J. Stangl, G. Bauer, J. M. Garcia, and P. M. Petroff, *Phys. Rev. Lett.* **85**, 1694 (2000).
40. L. C. A. Stoop and J. H. van der Merwe, *Thin Solid Films* **17**, 291 (1973).
41. Ya. I. Frenkel and T. Kontorova, *J. Phys. Acad. Sci. USSR* **1**, 137 (1939).
42. F. C. Frank and J. H. van der Merwe, *Proc. Roy. Soc. London, Ser. A* **198**, 205 (1949); **198**, 216 (1949).
43. J. H. van der Merwe, J. Woltersdorf, and W. A. Jesser, *Mater. Sci. Eng.* **81**, 1 (1986).
44. J. Tersoff, *Phys. Rev. Lett.* **56**, 632 (1986).
45. I. Markov and A. Trayanov, *J. Phys. C* **21**, 2475 (1988); *J. Phys.: Condens. Matter* **2**, 6965 (1990).
46. I. Markov, *Phys. Rev. B* **48**, 14 016 (1993).
47. F. H. Stillinger and T. A. Weber, *Phys. Rev. B* **31**, 5262 (1985); *ibid.* **36**, 1208 (1987).
48. Y. H. Xie, G. H. Gilmer, C. Roland, P. J. Silverman, S. K. Buratto, J. Y. Cheng, E. A. Fitzgerald, A. R. Kortan, S. Schuppler, M. A. Marcus, and P. H. Citrin, *Phys. Rev. Lett.* **73**, 3006 (1994).
49. T. Walther, A. G. Cullis, D. J. Norris, and M. Hopkinson, *Phys. Rev. Lett.* **86**, 2381 (2001).
50. A. Shklyaev, M. Shibata, and M. Ichikawa, *Surf. Sci.* **416**, 192 (1998).
51. B. Voigtländer and A. Zinner, *Appl. Phys. Lett.* **63**, 3055 (1993).
52. A. S. Bhatti, M. Grassi Alessi, M. Capizzi, P. Frigeri, and S. Franchi, *Phys. Rev. B* **60**, 2592 (1999).
53. A. Polimeni, A. Patane, M. Capizzi, F. Martelli, L. Nasi, G. Salviati, *Phys. Rev. B* **53**, R4213 (1996).
54. M. Colocci, F. Bogani, L. Carraresi, R. Mattolini, A. Bosacchi, S. Franchi, P. Frigeri, M. Rosa-Clot, and S. Taddei, *Appl. Phys. Lett.* **70**, 3140 (1997).
55. A. Bourret, C. Adelman, B. Daudin, J.-L. Rouvière, G. Feuillet, and G. Mula, *Phys. Rev. B* **63**, 5307 (2001).